GENERAL SYNTHESIS AND PROPERTIES OF SILVER NANOPARTICLES BY CHEMICAL REDUCTION METHOD

ALI M.ALI. HASSAN[a], E.A. ABDEL-AAL[b], MOUSTAFA F.BAKR[a], B.KH.DAMRANY[c]

(a) Chemistry , Faculty of Science, Al-Azhar University
(b) Central Metallurgical Research and Development Institute, CMRDI
(c) Chemistry Department, Faculty of Science, Al-Azhar University, Assiut branch

Abstract

Synthesis of silver nanoparticles which involves a number of steps occuring in the liquid phase. First, reduction of silver nitrate in presence of ammonia solution NH_4OH by strong reducing agent such as formaldehyde solution. The size and size distribution of the resulting silver nanoparticles prepared by chemical reduction are strongly dependent on the states of silver initial concentrations. Preliminary, the reduction of silver ions in aqueous solution generally yields colloidal silver with particle diameters of several nanometres. Initially, the reduction of various complexes with Ag^+ ions leads to the formation of silver atoms , which are followed by agglomeration into oligomeric clusters. These clusters eventually lead to the formation of colloidal Ag particles. Furthermore, by this method the effect of different reaction parameters such as silver initial concentration, the temperature, reaction time, pH of medium and the addition of some surfactants was studied . Silver nanoparticles prepared from this method will be more stable at room temperature. The crystallite size was found in the range of 70.3 to 84.6 nm and the average particle size of the silver nanoparticles was less than 800 nm. Samples were characterized in detail by X-ray diffraction (XRD), the morphology and also the particle size of silver nanoparticles was determined by Scanning Electron Microscopy (SEM).

Keywords:

Chemical Reduction, Silver Nanoparticles, X-ray diffraction (XRD),Scanning Electron Microscopy (SEM).

1. Introduction

In particular metal nanoparticles play an important role in many different areas. For example, they can serve as a model system to experimentally probe the effects of quantum confinement on electronic, magnetic, catalytic and other related properties [1]. They have also been widely exploited for use in photography [2], catalysis [3], biological labeling [4], photonics, optoelectronics [5], and information storage, surface-enhanced Raman scattering (SERS), and the formulation of magnetic Ferro fluids. The intrinsic properties of metal nanoparticles are mainly determined by their size, shape, composition, crystalline, and structure. In principle, any one of these parameters could be controlled to fine-tune the properties of metal nanoparticles [6]. The various metal nanoparticles have been widely investigated because they exhibit unusual optical, electronic, and chemical properties, depending

on their size and shape. This is opening for technological applications [7-9]. Nanoscale materials are of great interests due to their unique optical, electrical, and magnetic properties. These properties are strongly depend on the shape and the size [10-11]. . During the last two decades, many synthesis methods have been reported for the preparation of silver nanoparticles with tailor-made size, shape, and size controllability. In general, silver nanoparticles can be produced by various methods including the chemical reduction of silver ions with [12] or without [13] stabilizing agents, thermal decomposition in organic solvents [14], and photo reduction in reverse micelles [15-17]. Using these methods, silver nanoparticles with spherical, quasispherical, coalescence aggregates, hexagonal, cubic, wire, triangular.

Silver nitrate ($AgNO_3$ 99.9 %, pure chemical, Nice chemicals Pvt.Ltd.ochin - 682 Among prism, disc, triangular mark, belt, and shell shapes have been manufactured. All these advances have promoted the scientific knowledge on the nature of nanomaterial [18]. Shultz et al studied the effect of the size and shape on the spectral response of individual silver nanoparticles. They found that specific geometrical shapes give distinct spectral responses. The shape dependence of the optical spectra was obtained as a function of heat treatments [19].

In the present work, silver nanoparticles are prepared by the reduction of silver ions in presence of ammonia solution using the formaldehyde solution and without stabilizing agent. On the other hand, we also investigated the influence of the different parameters such as, initial concentration of silver ions, pH of medium, temperature, time, addition of surfactant, recovery, nature of stabilizers of reducing agent which control the size, morphology, shape, stability, colour, and physiochemical properties of the advanced nanomaterials. Therefore it is very important to enable to finely control the morphology of the nanomaterials.

2. Experimental

2.1. Materials

Chemicals were used as it is without any further purification. Calculated amount of $AgNO_3$ was dissolved in deionized water to prepare a proper Ag^+ ion concentration. Ammonium hydroxide solution (NH_4OH, 33%, Adwic, Egypt), formaldehyde solution HCHO (37% wt sol in water, stable with 10-15 % methanol, d = 1.083, B.p = 93) was purchased from El Nasr pharmaceutical, Sodium Dodecyl Sulphate SDS ($C_{12}H_{25}O_4S.Na$, MW = 288.5 Critical Micelle Concentration (CMC) 6 to 8 mM 0.1728 to 0.2304%, and 15 to 30 C°) was purchased from SERVA Company, Hexadecyl pyridinium chloride HPC (98% assay $C_{21}H_{38}Cl$ N. H_2O warning irritates skin and eyes) were purchased from Alfa Aesar A Johnson Matthey
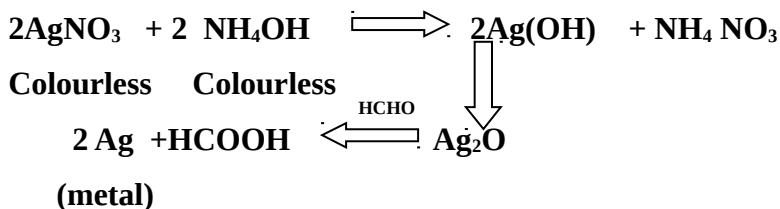
Company and Triton (cloud point 23 C°, average molecular weight ~ 537 based on 7.5 ethylene oxide units and d = 1.058 gm/ml at 25 C°) .

n=7-8
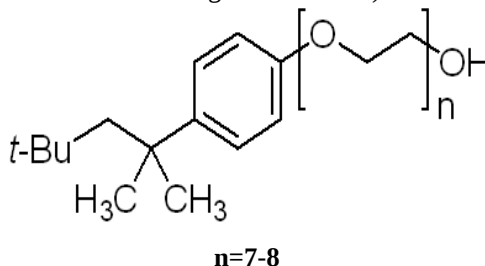
The Triton Structure

2.2. Synhesis procedure

We used a simple method to prepare nanometere-sized silver through the reduction of $AgNO_3$ by reducing agent such as formaldehyde solution in the presence of ammonia solution. Solution A was prepared by dissolving $AgNO_3$ (1.7gm) in 50 ml deionized water this solution is colourless. Solution B is ammonia solution. Solution C is formaldehyde solution. 5 ml from solution B was injected in to solution A at room temperature under stirring. When the ammonia solution reacts with silver nitrate solution produced intermediated step from silver oxide have black brown colure is formed with in a few second which then transforms into stable product from silver hydroxide colorless.

$$2AgNO_3 \; + 2 \; NH_4OH \; \Longrightarrow \; 2Ag(OH) \; + NH_4 \, NO_3$$

Colourless   **Colourless**

$$2 \, Ag \; + HCOOH \; \overset{HCHO}{\Longleftarrow} \; Ag_2O$$

(metal)

In order to prevent the introduction of NO^-_3 in the reaction system, the mixture of solution A and B containing silver hydroxide and silver oxide would be reduced by adding 10 ml of solution C at room temperature under stirring to form a precipitated powder of silver metal particles (white brown). These particles are dried at room temperature. During the course experiments, the change in colour of silver nanoparticles was measured to follow up the change of reaction products with the change of the reaction parameters. On the other hand, the influence of different reactions parameters such as the effect of silver initial concentration, reaction time, temperature, the recovery of silver nanoparticles, pH medium, crystallite size and the polymer additions was studied.
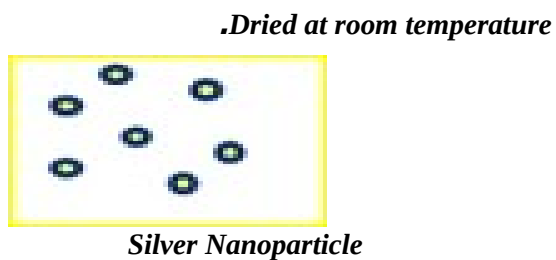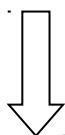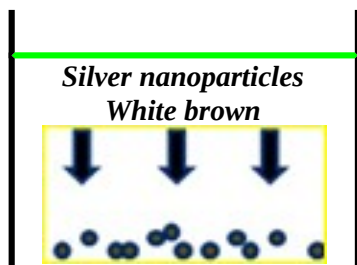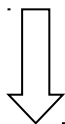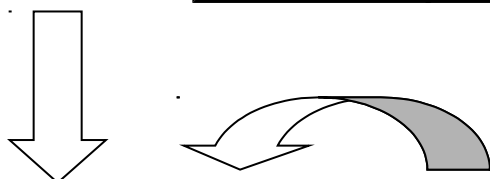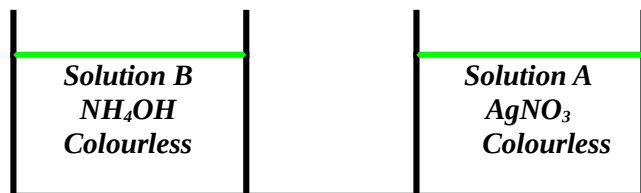
**Diagram of preparation methods of silver nanoparticles obtained in aqueous
solutions.**

2.3. Samples characterization

2.3.1. *Crystal structure and phase analysis*

Phase identification, purity, relative crystallinity and crystallite size of the products were performed at room temperature using X-ray diffractometer equipped with an automatic divergent slit (XRD; Philips PW1700 diffractometer, Netherlands). Diffraction patterns were obtained using Cu- Kα radiation (λ= 0.15418 nm) and a graphite monochromator in the 2Ө range from 10˚ to 80˚. XRD patterns were fitted using pseudo lorentzian line shapes for accurate determination of lattice constant and apparent crystallite size. On the other hand, X-ray diffraction analysis was performed on some selected deposited silver particle samples at different experimental conditions. Phase identification of the examined samples was carried out using JCPDS cards (Joint Committee for Powder Diffractions). Purity was identified from the percentage of present phases calculated from XRD data.

2.3.2. *Morphology*

Morphology of the synthesized nanocomposites was analyzed using scanning electron microscopy (SEM, JEOL-JSM-5410, Japan) operating at 30.0 kV. SEM was used to investigate the morphology of some selected deposited silver particle samples; degree of agglomeration of the deposited silver particles was also estimated from the SEM images compared with the crystallite size data obtained from XRD results. Moreover, Transmission electron microscopy (TEM; JEOL JEM-1230) operating at 120 kV was also performed on some selected samples to investigate the silver particle size and crystal structure.

2.3.3 *Chemical Analysis*

Wet chemical analysis of some selected deposits samples was performed to investigate the silver ion concentration of the deposited samples to calculate the purity of particles. The analysis was performed using the titration of the solution after precipitation to determine the silver dissolved in solution by using sodium chloride and potassium chromate to calculate the recovery percentage of silver nanoparticles.

Calculation

The calculation was done according to the following equation

Recovery of precipitated silver =
$$\frac{\text{Wt. of precipitated silver}}{\text{Wt. of theoretical silver}} \times 100$$

3. Results and discussion

3.1. The Effect of Silver Initial Concentration:

Silver nanoparticles were synthesized according to the method described in the previous section, the reduction of $AgNO_3$ by the formaldehyde solution in presence of ammonia solution which   reacts with silver nitrate solution yielding an intermediate step of silver oxide with a blackish brown colour in a few seconds to silver hydroxide which then transforms into stable product of silver nanoparticles.

Table 1. Synthesis of silver nanoparticles at different initial concentrations

Concentration (g/l)	Recovery (%)	Crystallite Size (nm)
0.42	100.00	80.50
0.85	99.60	75.50
1.70	98.86	70.30
5.10	98.27	84.60
8.48	98.00	72.70

Examination of the results cited in Table 1 reveals that the variation of recovery of silver nanoparticles and the variation of crystallite size (nm) at different silver initial concentrations. In a typical procedure, small silver nanoparticles were first synthesized in aqueous solution by reduction of silver nitrate solution (colourless) with formaldehyde solution in presence of ammonia solution to form precipitated powder of silver metal particles (white brown), which are dried at room temperature.
Th   e
si   .

3.

                                                                                                   l
co   s
ar   .
sti   n
te   e
as   .
O   ₂
or   e
pc

| A (2.47×10 moll^{-1}) |
| B (5×10^{-3} moll^{-1}) |
| C (1×10^{-2} moll^{-1}) |
| D (3×10^{-2} moll^{-1}) |

D

C

B

A

Fig.1. XRD patterns of silver powder precipitated at different initial concentrations of silver nitrate solutions containing, pH 6.3 of solution, 5 min. stirring, and 35 Cº.

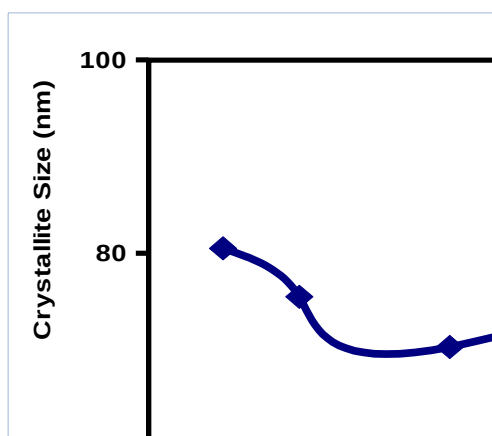*3.3. Influence of Crystallite Size of Silver Nanoparticles:*

Fig.2. Variation of crystallite size of silver nanoparticles versus silver initial concentrations at pH 6.3 of solution, 5 min stirring at 35 Cº.

Fig.2. shows that when the silver initial concentrations increase the crystallite size of silver nanoparticles decrease. .As shown in Table 1, the increase of silver initial concentrations leads to decrease the crystallite size of silver nanoparticles except at 5.1g/l silver initial concentration.

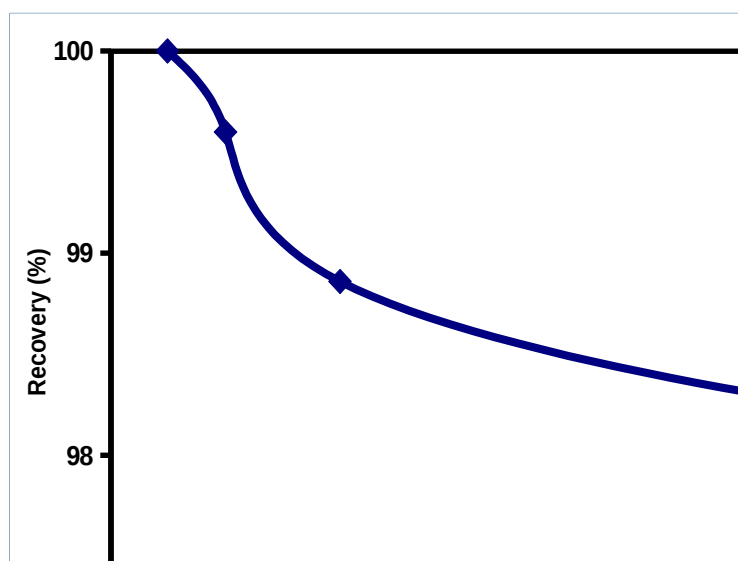*3.4 Influence of Recovery of Silver Nanoparticles*:

Fig.3. Variation of the percentage (%) of recovery of silver nanoparticles versus silver initial concentrations at pH 6.3 of solution, 5 min. stirring at 35 Cº.

It is obvious that, from Table.1 and Figure 3**,** the silver initial concentrations affect the recovery of silver nanoparticles. When the silver initial concentrations increase the recovery of silver nanoparticles decrease gradually due to the silver in the solution increases by increasing the concentration which increases the recovery of silver nanoparticles.

3.5. Influence of Morphology of Silver Nanoparticles

It is well known that the morphology and size distribution of metallic particles produced by the reduction of silver hydroxide solution depend the on the various reaction conditions such as silver initial concentrations, temperature, the time, pH of solution, mode and order of addition of surfactants.
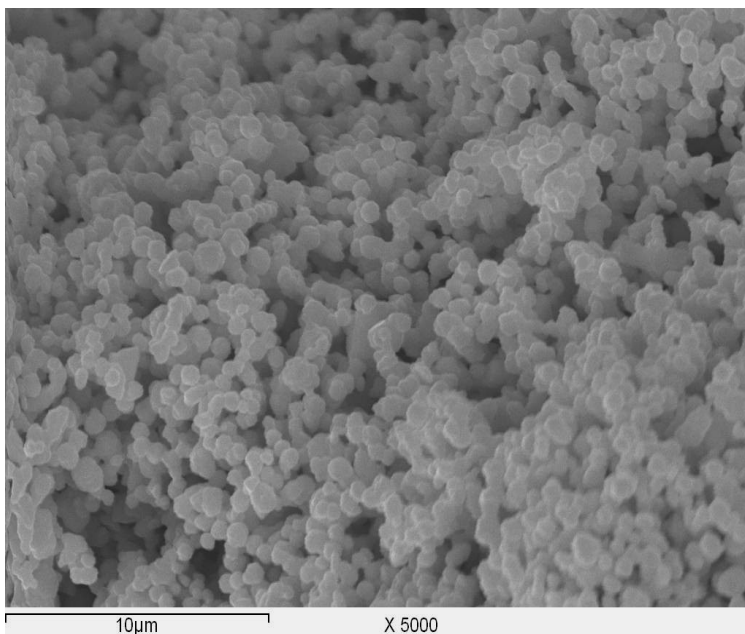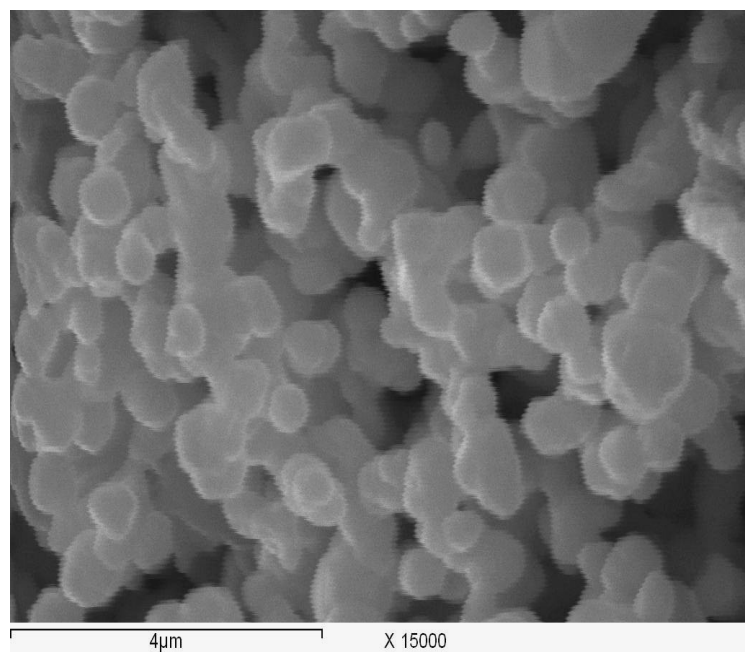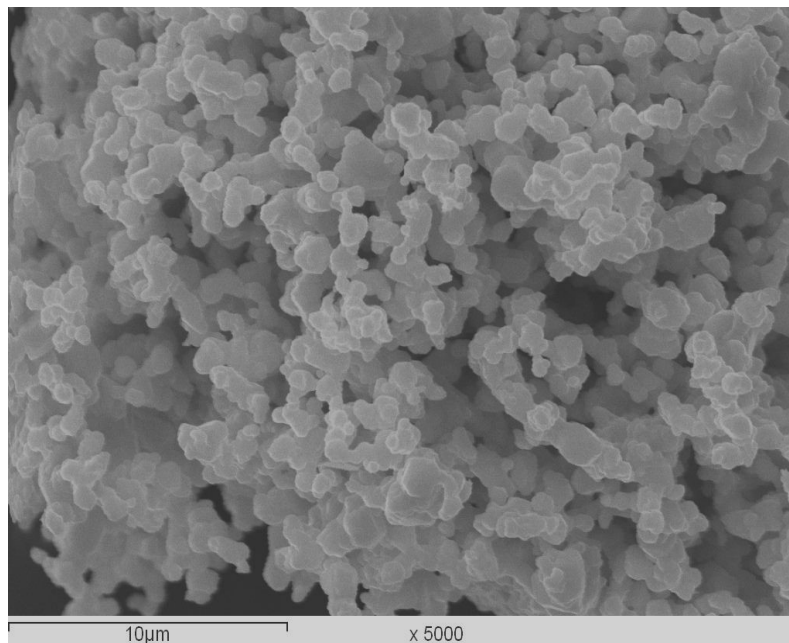
Fig. 4 (A, B) SEM images of silver powders precipitated from solutions containing 0.85 g/l (5 x 10^{-3} mol) AgNO$_3$ at 35 C°, and pH 6.3 of solution.
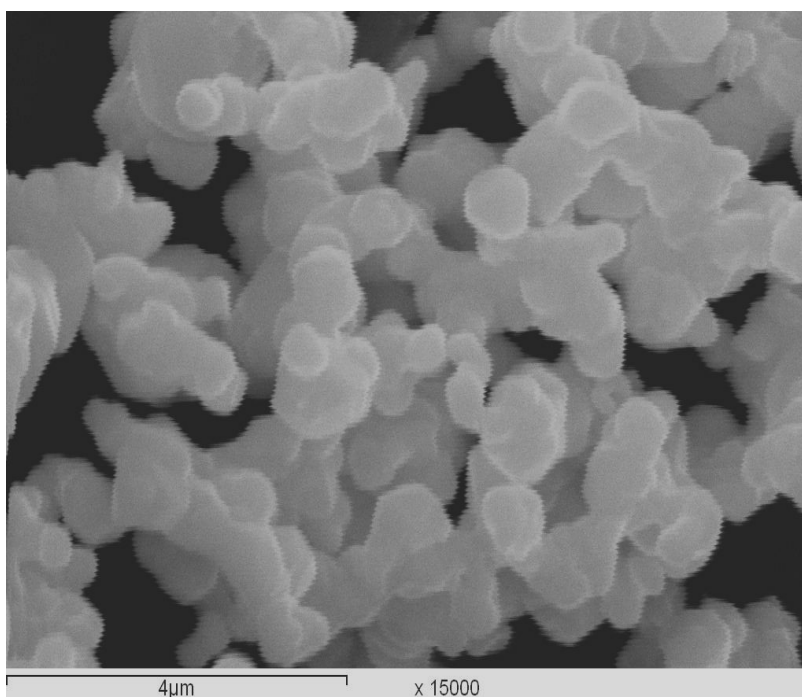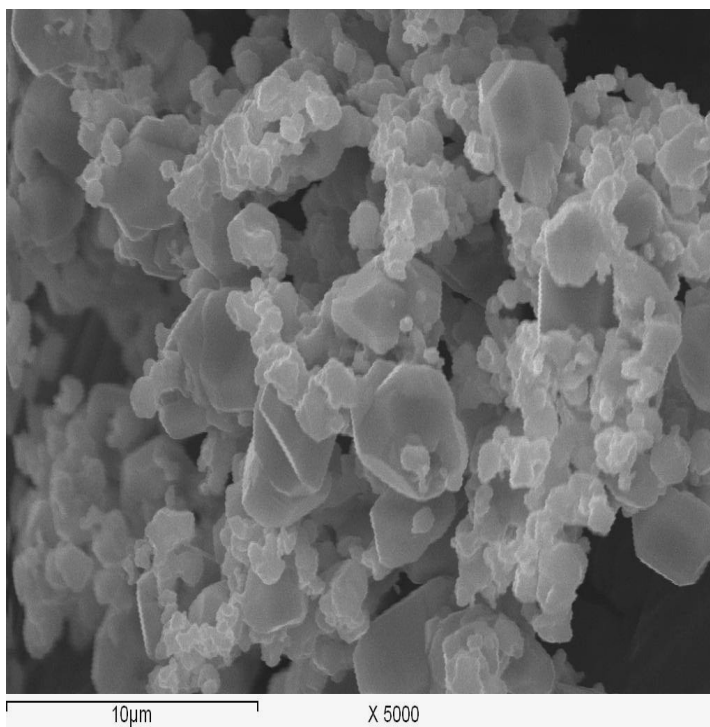
ALI M.ALI. HASSAN, *et al*

C

D

Fig.5 (C, D) SEM images of silver powders precipitated from solutions containing 1.70 g/l (1 x 10^{-2} mol) AgNO$_3$ at 35 C°, and pH 6.3 of solution.
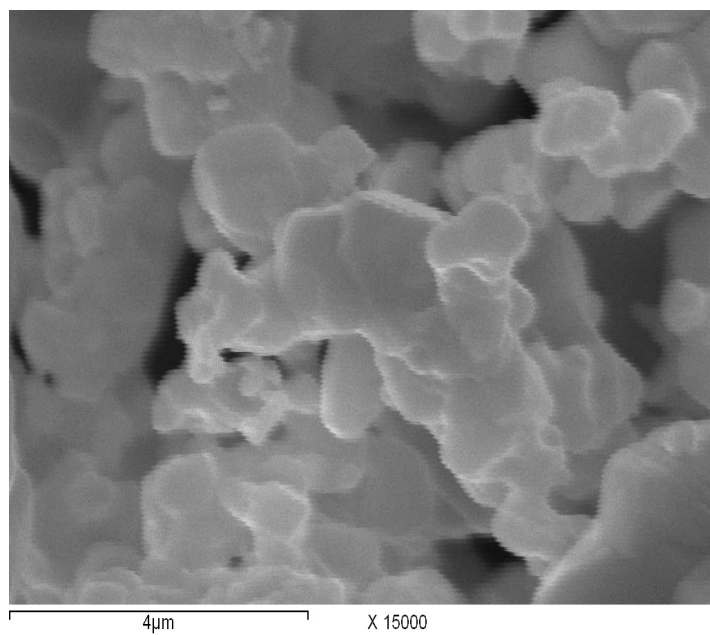
E

10μm   X 5000

F

4μm   X 15000

Fig. 6 (E, F) SEM images of silver powders precipitated from solutions containing 5.1 g/l $(3 \times 10^{-2}$ mol) AgNO$_3$ at 35 C$^\circ$, and pH 6.3 of solution.

ALI M.ALI. HASSAN, *et al*

The mean particle size and the standard deviation of the resulting Ag particles obtained at each set of synthesis conditions are also present, together with figure number identifications for the corresponding particles. Figures (4-6) show SEM images of the precipitated silver powders from solution containing 0.85,1.70 and 5.1 g/l ,$AgNO_3$ at 35 C°, and pH 6.3 of solution. On the other hand, this method could not produce uniform silver nanoparticles in high yields. Figure 4 (A, B) illustrates the morphology of silver(at 0.85 g/l (5 x 10^{-3} mol) $AgNO_3$ at 35 C°, and pH 6.3 of solution) which shows quasispherical and cubes shape with particle size range from 500-800 nm. This indicates that the particles are agglomerated together to form coalescence aggregates. Figure 5 (C, D) shows the morphology of silver(at 1.70 g/l (1 x 10^{-2} mol) $AgNO_3$ at 35 C°, and pH 6.3 of solution) quasispherical and cubes shape and the average particles size in the range 400 - 800 nm. On the contrary, Figure 6 (E, F) shows the morphology at high silver initial concentration (5.1 g/l (3 x 10^{-2} mol) $AgNO_3$ at 35 C°, and pH 6.3 of solution), the particles are agglomerated together to form coalescence aggregates shape.

3.6 Influence of addition of surfactant

3.6.1 Influence of addition of Anionic Surfactant (SDS)

From another point of view, the effect of addition of anionic surfactant Sodium Dodecyl Sulfate (SDS) was studied on the recovery, crystallite size and morphology of silver nanoparticles. Furthermore, on carrying out the experiment including the solution containing 0.4 M silver nitrate in presence of ammonia solution and Formaldehyde, 25 ml anionic surfactant (SDS), 5 min. stirring, 35 C° and pH 4.65 of solution. On other hand, the recovery of silver nanoparticles was found 99.81%. By Figure, 7 the XRD characterization of the powder produced, contain only pure silver nanoparticles of size 71.1 nm. Hence the addition of anionic surfactant SDS has a great effect on the morphology of deposited silver nanoparticles where it greatly changes from quasispherical and cubes shape (see figure 4 (A, B)) to uniform rod- like structure (see Figure10(A, B)).

Fig. 7 XRD patterns of silver powder precipitated at different experimental conditions for solutions containing, 0.4 M from silver nitrate, 25 ml from anionic surfactant (SDS), 5 min stirring, 35 Co and pH of solution 4.65.

3.6.2 Influence of addition of Cationic Surfactant (Hexadecyl Pyridinium Chloride):

Fig.7 XRD patterns of silver powder precipitated at different experimental conditions for solutions containing, 0.4 M silver nitrate, 25 ml anionic surfactant (SDS), 5 min. . stirring, 35 C° and pH 4.65 of solution

Cationic surfactant is adsorbed strongly onto most solid surfaces which is more expensive than anionic or nonionic and it has poor suspending power for carbon. On the other hand, the solution under study containing 0.4 M silver nitrate in presence of ammonia solution and Formaldehyde, 25 ml cationic surfactant (Hexadecyl pyridinium choloride), 5 min. stirring, 35 C° and pH 5.2 of solution. Hence we studied the addition of the cationic surfactant on the recovery, crystallite size and morphology of silver nanoparticles.. The recovery of silver nanoparticles was found 99.85 %. As shown in Figure 8 , the XRD data show the formation of silver chloride with silver nanoparticles. However, these powders containing two phases which they are silver and silver chloride of size 148.9 nm.

Fig. 8 XRD patterns of silver powder precipitated at different experimental conditions for solutions containing, 0.4 M silver nitrate, 25 ml cationic surfactant (Hexadecyl pyridinium chlorides), 5 min stirring, 35 Cᵒ and pH 5.2 of solution.

3.6.3   *Influence of addition of Nonionic Surfactant (Triton):*

Nonionic surfactants are available as 100 % active material free of electrolyte. They are resistant to hard water but at high concentrations, they are soluble in water and organic solvents including hydrocarbons. In a typical procedure, the effect of addition nonionic surfactant was studied on the recovery, crystallite size and morphology of silver nanoparticles from the solution under study. The recovery of silver nanoparticles was 99.75, and the crystallite size was 117.6 nm as shown in Figure 9. On the other hand, according to SEM image (as shown in figure !0) , the addition of nonionic surfactant on the morphology of silver naonpowder cleared that, the morphology of silver nanoparticles changed from cubic structure to face center cubic structure (FCC).
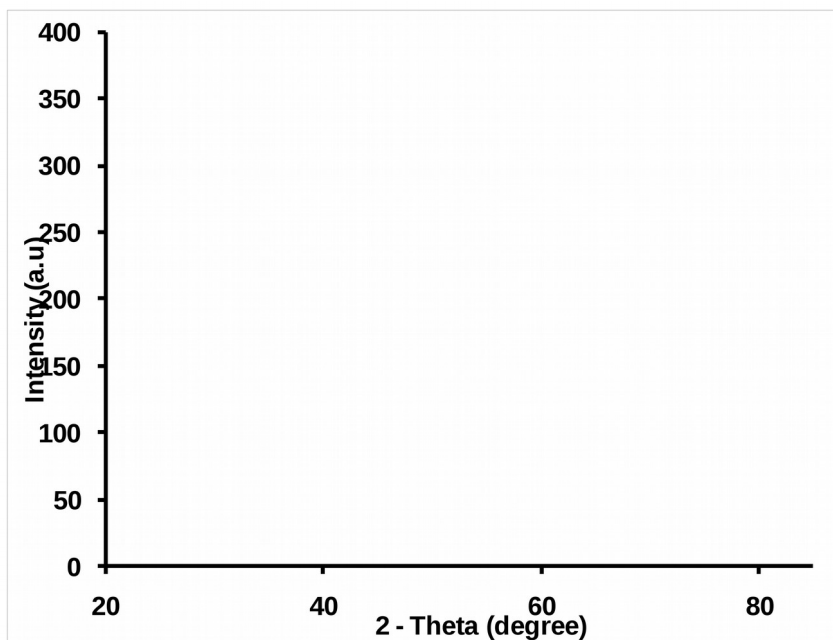
Fig. 9 XRD patterns of silver powder precipitated at different experimental conditions for solutions containing, 0.4 M silver nitrate, 25 ml nonionic surfactant (Triton), 5 min stirring, 35 Cº and pH 5.53 of solution.
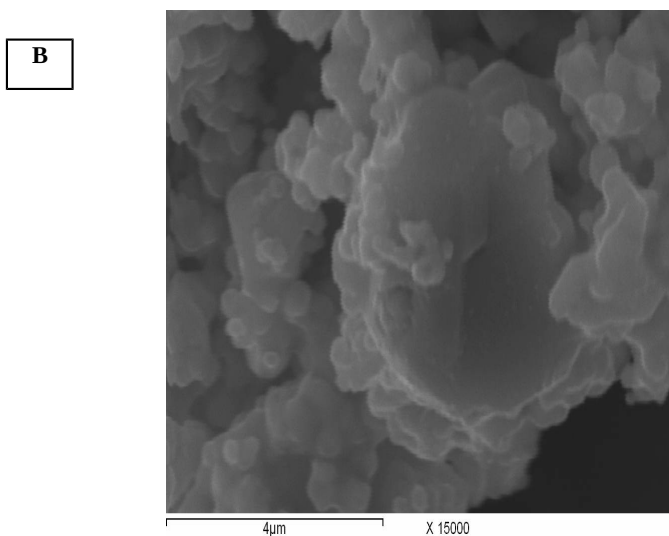

Fig. 10 (A, B) SEM images of silver powders precipitated from solutions containing 0.4 M silver nitrate, 25 ml nonionic surfactant (Triton), 5 min. stirring, 35 Cº and pH 5.53

4. Conclusion

Silver nanoparticles were successfully synthesized through reduction of silver ions in aqueous solution yielding colloidal silver with particle diameters of several nanometers. Initially, the reduction of various complexes with Ag+ ions leads to the formation of silver atoms which followed by agglomeration into oligomeric clusters. These clusters eventually lead to the formation of colloidal Ag particles. Furthermore, in this method , the effect of different reaction parameters, i.e. by Increasing the silver initial concentrations, recovery of silver nanoparticles will decrease gradually from 100% to 98%, the crystallite size of silver nanoparticles will also decrease then it increases and after that decreases again. On the other hand, the morphology obtained by this method was non-uniform silver nanoparticles, in high yields (quasispherical, cubes and coalescence aggregates shape) and the particle size in the range of 400-800 nm. Also, the effect of added anionic surfactant is greatly changed the morphology of deposited silver nanoparticles from cubic spherical structure to uniform rod- like structure, and also the nonionic surfactants greatly changed the morphology from cubic structure to face centred cubic structure (FCC).

References

1. M. A. El-Sayed. Acc. Chem. Res. 34 (2001) 257.
2. M.P. Pileni. Adv. Funct. Mater. 11(2001) 323.
3. S. Nie, S. R. Emory. Science 275(1997) 1102.
4. P. V. Kamat. J. Phys. Chem. B 106 (2002) 7729.
5. S. A. Maier, M. L. Brongersma, P. G. Kik, S. Meltzer, A. A. G. Requicha, H. A.AtwaterAdv. Mater. 13(2001) 1501.
6. Y. Sun,Y. Xia Science 298 (2002)2176.
7. Y. Sun, Y. Yin, B. T Mayers, T. Herricks, Y. Xia. Chem. Mater. 14 (2002) 4736.
8. D. Zhang, L. Qi, J. Yang, H. Cheng, L. Huang. Chem. Mater. 16 (2004) 872
9. 9-L.Suber,I. Sondi, E. Matijevic, D. V. Goia J. Colloid Interface Sci. 288 (2005)489.
10. Y.W. Cao, R. Jin, C.A. Mirkin, J. Am. Chem. Soc. 123 (2001) 7961.
11. F. Kim, J.H. Song, P. Yong, J. Am. Chem. Soc. 124 (2002) 14316.
12. N. Toshima, T. Yonezawa, K. Kushihashi J. Chem. Soc. Faraday Trans. 89 (1993)2537.
13. L. M. Liz-Marzan, A. P. PhilipseJ. Phys. Chem. 99 (1995) 15120.
14. K. Esumi, T. Tano, K. Torigoe, K. Meguro. Chem. Mater. 2 (1990)564.
15. F. Mafune, J. Y. Kohnok, Y. Takeda, T. Kondow J. Phys. Chem. B 104 (2000) 8333.
16. H. H. Huang, G. L. Loy, C. H. Chew, K. L. Tan, F. C. Loh, J. F. Deng, G. Q. Xu Langmuir 12 (1996) 909.
17. M. P. Pileni, I. Lisiecki, L. Motte, C. Petit, J. Cizeron, N. Moumen, P. Lixon Prog. Colloid Polym. Sci. 93 (1993) 1.
18. T. Dadosh. Materials Letters 63 (2009) 2236–2238.

19. J. J. Mock, M. Barbic, D. R. Smith, D. A. Schultz, and S. Schultz, J. Chem. Phys. 116 (2002) 6755-6759**.**